RSC Advances

ROYAL SOCIETY OF CHEMISTRY

www.rsc.org/advances

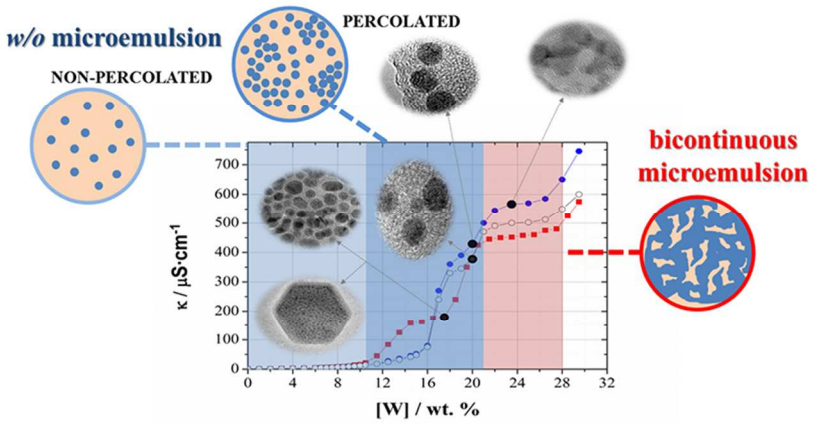

Graphical Abstract
83x35mm (300 x 300 DPI)

Journal Name

RSCPublishing

ARTICLE

Electrosynthesis method of CoPt nanoparticles in percolated microemulsions

Cite this: DOI: 10.1039/xoxxooooox

A. Serrà, E. Gómez and E. Vallés*.

Received ooth January 2012,
Accepted ooth January 2012

DOI: 10.1039/xoxxooooox

www.rsc.org/

An electrochemical synthesis of CoPt nanoparticles on Si/Ti/Au substrates has been performed in percolated water-in-oil (*w/o*) microemulsions to define the nanoparticle size and composition. The results allowed us to propose this method for direct growth of nanoparticles over substrates, avoiding overlapping of the particles during the deposition. We use proportions of aqueous CoPt solution, surfactant and oil components to form *w/o* microemulsions in which droplets of aqueous solution could be dispersed in the oil, but in percolated state, to enhance the global conductivity of the system, allowing the electrodeposition process, although at moderate rate. In this conditions isolated nanoparticles have been obtained, which composition is depending on the composition of the solution of the aqueous droplets. Nanoparticles obtained at very low deposition rate aggregate by superficial diffusion leading to some well-defined hexagonal particles, reflecting their crystalline structure. When the proportions of the microemulsion components lead to bicontinuous structure, growing particles overlap and branched structures have been obtained by electrodeposition.

1. Introduction

Various methods for controlling the growth of nanoscale materials (nanoparticles, nanorods or nanowires) of semiconductors, metals, and oxides have been developed, some of them to synthesize alloys or intermetallic nanoparticles, [1-4] usually by means of chemical reduction in micelles. Defined shape, composition and crystal phase of the nanoparticles is essential for catalytic, optical, chemical and magnetic applications.[5,6] Thermal treatments at high temperatures are often necessary to obtain a specific crystal phase of the alloy particles but these post-synthesis treatments often affect the size, structure and particle distribution of particle's sizes.[7]
Although electrodeposition, low cost and simple technique, has shown as a useful technique to prepare nanoscale materials that can be grown directly over devices[8-10] and allows preparing nanostructures using templates or photolithographed substrates.[11-13] Furthermore, it requires a strict control of the deposition charge to grow nanoparticles over substrates. However, electrodeposition could be used to nanoparticles controlled synthesis with appropriate nanotemplates. Specific microemulsions could be used for this aim. Different types of microemulsions with water, oil and surfactants can be formed[14-17]: oil-swollen direct micelles dispersed in water (*o/w* microemulsions), water-swollen inversed micelles dispersed in oil (*w/o* microemulsions), or with both aqueous and oily interconnected domains (bicontinuous microemulsions).[18-20] *W/o* microemulsions have been frequently used to form small nanoparticles by chemical reduction in the droplets.[21-23] Moreover, some recent studies have been demonstrated the possibility to use also microemulsions as templates for electrochemical synthesis of nanostructures, without using aggressive reagents like hydrazine or borohydride. The very low conductivity of the w/o microemulsions makes very difficult the electrodeposition, but bicontinuous microemulsions (more conductive) allows electrodepositing porous or non-continuous deposits.[24-26] We propose now the use of percolated microemulsions (moderate conductivity) to electrodeposit nanoparticles of controlled and variable sizes.
The aim of this work is the synthesis of CoPt nanoparticles of variable size, shape and composition by electrodeposition in percolated water-in-oil microemulsions, with enough conductivity to permit electrodeposition. Percolated microemulsions can guarantee the droplets independence. The droplets should contain the electrolytic solution and the control of the size and distribution of the droplets would provide nanoparticle of controlled size, shape and distribution. In order to vary the microemulsion structure, different [Co (II)] / [Pt (IV)] ratios have been studied. The CoPt system has been selected because CoPt nanoparticles present increasing interest for their catalytic or magnetic properties and the proposed method could permit the preparation of controlled size and shape NPs.

2. Experimental section

The microemulsion (ME) region in the Diisopropyl Adipate (O), Triton X-100 (S) and aqueous solution (W) system was determined

by the stepwise addition of aqueous solution to oil/surfactant mixtures at 25ºC, under stirring (100 rpm). The samples were homogenized (Vortex) and analysed once equilibrium was reached. The aqueous phase contains $CoCl_2$ (2.5 mM, 7.5 mM $CoCl_2$ or 10.0 mM $CoCl_2$) + 1.2 mM Na_2PtCl_6 + 0.1 M NH_4Cl + 10 $g \cdot dm^{-3}$ H_3BO, solutions, freshly prepared with water treated with a Millipore Milli Q system. The solution's pH was adjusted (pH = 4.5) with NaOH solutions. The solubility of the salts in the oil was negligible. The microemulsions type was determined by different dyes (Black Sudan HB and Rhodamine B) and conductivity measurements that were carried out using a Crison conductimeter GLP31. The conductivity cell was a model 52-92 (Crison) with Pt electrodes and a cell constant of $1cm^{-1}$.

Electrochemical study and deposits preparation were performed in a conventional three-electrode cell at room temperature. A potentiostat/galvanostat Autolab with PGSTAT30 equipment and GPES software was used. Each system was de-aerated by argon bubbling before each experiment and maintained under argon atmosphere during the study. Silicon / Ti (1000 Å) / Au (500 Å) substrates (0.5 cm x 0.5 cm) supplied by IMB-CNM (CSIC) have been used as working electrodes to obtain the deposits. The substrates were cleaned with ethanol, rinsed in water and dried before electrodeposition. The reference electrode was an Ag/AgCl/1M KCl electrode. The counter electrode was a platinum spiral. The microemulsions did not stir during the electrodeposition process to maintain the microemulsion structure as template.

Elemental composition of the deposited nanostructures was measured using an Electron Probe Micro-Analysis (EPMA) by Wavelength-Dispersive X-Ray spectroscopy analysis (WDS) with Camera SX-50 equipment. Both Hitachi H-4100FE (Field Emission Scanning Electron Microscopy FE-SEM) and Hitachi 800 MT TEM were used for the observation of the different samples.

3. Results and discussion

3.1. Selection of the best microemulsions to perform the CoPt electrodeposition

Different proportions of the three selected components (oil, surfactant and aqueous electrolytic solution) were tested to define the proportions able to prepare microemulsions. From these, the most conducting ones were chosen to try performing confined electrodeposition of CoPt nanostructures. The crystals liquids zone was avoided to perform the deposition, due to the difficulty of working in too much viscous medium.

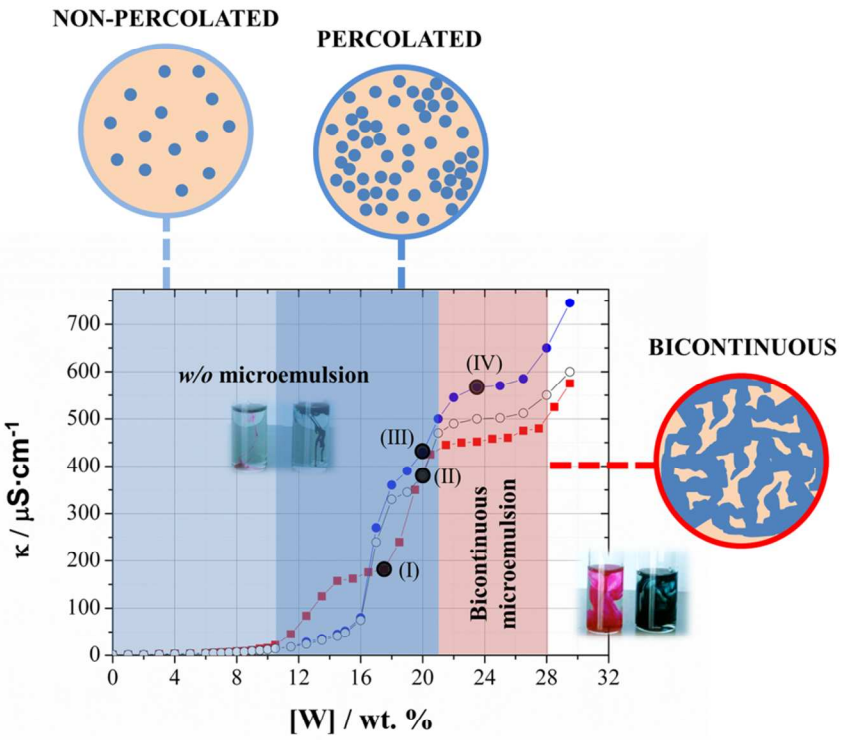

Fig. 1 Conductivity (κ) as a function of aqueous solution content (w) at 25 ºC for samples with a S: O ratio of 0.59 and different concentration of $CoCl_2$: (■) 2.5 mM, (○) 7.5 mM and (●) 10.0 mM

From measures of conductivity of the O:S:W systems, the observation of their stability, and the test with two different dyes (Black Sudan and Rhodamine B), the microemulsion regions have been identified. Fig. 1 shows the curves of conductivity of the ternary system with a constant S:O ratio of 37:63(0.59) and variable percentage of aqueous solution, for three different compositions of the electrolytic solution (*w*). In each case, the conductivity increases with the percentage of aqueous solution, showing two significant changes, the first one interpreted as the change from the continuous *w/o* microemulsion to the percolation of aqueous droplets, and the second one as the change from percolated microemulsion to bicontinuous microemulsion[24,25]. Further increase of the *w*

percentage causes the separation of phases, reflected by the new increase of conductivity. The use of the two dyes verified the results obtained by conductivity measures. At low content of aqueous solution, the diffusion of the Black Sudan (lipophilic dye) is faster than that of the Rhodamine B (hydrophilic dye), which suggests that the microemulsion is *w/o* type. By increasing significantly the content of aqueous solution, a similar and fast diffusion rate of the two dyes was observed, which is coherent with a bicontinuous microemulsion structure.

The microemulsion regions were affected by the composition of the aqueous component (*w*). An increase of [$CoCl_2$] in the aqueous component leads to a change in the microemulsions structure, attributed to interfacial effects (e.g., modification of interfacial tension, variations in the interfacial rigidity). For the same content of aqueous solution (for example, a 15 wt. % of *w*), a higher conductivity of the microemulsion with 2.5 mM of $CoCl_2$ than that of the systems containing triple or quadruple [$CoCl_2$] is observed (Fig.1), which demonstrates that the change in the internal structure of the microemulsion is the dominating effect on the conductivity, because the increase of ions concentration do not justifies these values.

3.2. Voltammetric study of the CoPt process in the microemulsions.

From the earlier results, three percolated water-in-oil microemulsions (points **I**, **II** and **III** in Fig. 1) and one bicontinuous (point **IV** in Fig. 1) were selected to perform the CoPt electrodeposition. The composition of these microemulsions is shown in Table 1. The voltammetric response of the process in each microemulsion was analysed and interpreted by comparing with those obtained in aqueous solution without and with surfactant.

Table 1. Microemulsion composition of different studied systems.

ME	wt. % O	wt. % S	wt. % w	S:O ratio	[$CoCl_2$] in *w* mM	$Na_2[PtCl_6]$ in *w* mM
I	51.6	30.4	18.0	0.59	2.5	1.2
II	50.4	29.6	20.0	0.59	7.5	1.2
III	50.4	29.6	20.0	0.59	10.0	1.2
IV	48.1	28.4	23.5	0.59	10.0	1.2

In the Fig. 2a, the voltammetry of the CoPt system in the aqueous solution selected reveals the initial platinum reduction (R_1), followed by proton reduction (R_2); cobalt co-deposition takes place simultaneously to hydrogen evolution (R_3, from about -0.5 V). Oxidation of retained molecular hydrogen (O_1) and CoPt alloy (O_2) were observed in the anodic scan. The superficial oxidation of the initial platinum was detected at potentials more positive than 0.5 V (O_3).

When the voltammetric curves of CoPt in aqueous solution containing significant concentration of surfactant were recorded (Fig. 2b), some changes were observed: the platinum reduction process begins at more negative potentials as a consequence of the adsorption of the surfactant on the gold substrate. The protons reduction and the hydrogen evolution were also minimized by the presence of the surfactant adsorbed on the substrate. In the anodic scan, the peak O_2, corresponding to alloy oxidation, is clearly observed. The adsorption of the surfactant avoids also the formation of superficial platinum oxides. Therefore, CoPt can deposit in the presence of significant amount of surfactant.

In the microemulsion system **I**, the voltammetric curves reflected very lower current density than that observed in aqueous solution containing surfactant, as corresponds to the lower amount of aqueous solution (containing the electroactive species) and the specific microemulsion structure (Fig. 2c). Slow reduction processes (reflected by the low current density/potential slope) took place as a consequence of the low conductivity of the system.

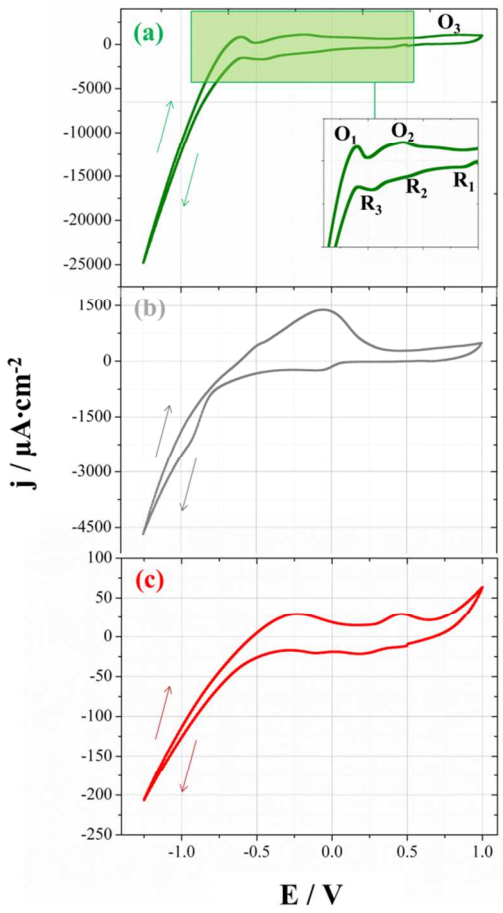

Fig. 2. Cyclic voltammograms of (a) aqueous solution, (b) aqueous solution with Triton X-100 (30.4 wt. %) and (c) microemulsion **I,** 50 $mV \cdot s^{-1}$. Si/Ti/Au substrate.

Fig. 3 analyses the effect of the [$CoCl_2$] (in the aqueous component *w* of the microemulsion) in the electrodeposition process, by comparing the voltammetric curves of the microemulsions I, **II** and **III**. When the [$CoCl_2$] increases, the cobalt reduction current increases and the alloy oxidation peak enhances. Only one oxidation peak was observed, which reflects the formation of a CoPt solid solution, for the different [Co(II)]/[Pt(IV)] ratios in solution. The increase of the [$CoCl_2$] in the aqueous solution also increases the conductivity of the global deposition system, respect to that of microemulsion **I**, which minimizes the ohmic control of the process.

The voltammetric results demonstrate that the deposition process of CoPt in percolated *w/o* microemulsions is feasible, with similar behaviour that in aqueous solution containing surfactant, but at lower deposition rate.

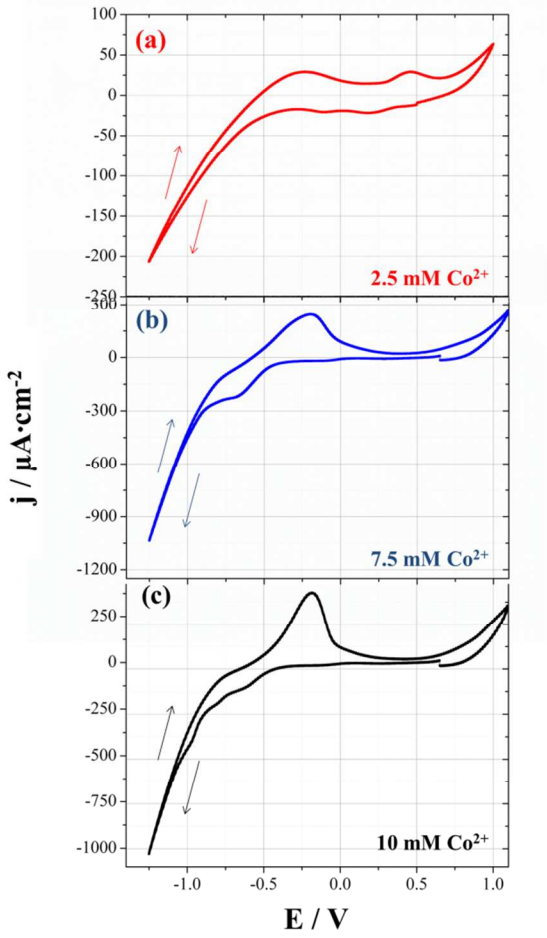

Fig. 3. Cyclic voltammograms of CoPt in microemulsions: (a) **I**, (b) **II** and (c) **III**.

3.3. Preparation and characterization of the CoPt deposits.

From the previous voltammetric study, Pt and Co codeposition seems to be possible from the tested microemulsions. Deposits were potentiostatically prepared, by applying low deposition charges to obtain CoPt nanoparticles and to analyze the first stages of the deposition process in percolated microemulsions. All the deposits were obtained without stirring to maintain the confined electrodeposition process in the microemulsion template. Hydrogen bubble detachment during electrodeposition was not observed, which corroborates the information obtained in the voltammetric study.

Deposits were analysed and observed for SEM and TEM. For TEM observation, the nanostructures were detached from the substrate. This was achieved by removing the Au layer using a saturated I_2 / I^- solution. The nanostructures were later retained by an external magnetic field and washed with water and ethanol.

Clear differences in the Pt percentage were detected at fixed deposition potential (-1050 mV) and charge density (300 mC·cm^{-2}) for the studied microemulsions (Table 2), due to the different concentration of Co (II) in the aqueous component.

Table 2. Elemental composition of CoPt deposits (WDS analysis) prepared at 25 °C in different microemulsion systems.

ME	[$CoCl_2$] in *w* at. %	$Na_2[PtCl_6]$ in *w* at. %	at. % Co	at. % Pt
I	68	32	59 ± 1	41 ± 1
II	86	14	76 ± 1	24 ± 1
III	89	11	77 ± 1	23 ± 1
IV	89	11	77 ± 1	23 ± 1

From microemulsion **I**, CoPt deposits of around 41 at. % of Pt were obtained. FE-SEM and TEM micrographs (Fig. 4) show that these deposits are constituted by small nanoparticles of a few nanometers (Fig. 4a, 4c) with a narrow particle distribution size around 4 nm (Fig. 4d), and aggregates of nanoparticles in the form of hexagonal structures (Fig. 4a, 4b). Confined nanoparticles can aggregate by diffusion on the substrate in well-defined hexagonal structures. This defined shape leads to propose the formation of deposits with hcp-cobalt crystalline structure distorted by platinum incorporation, as occurs in aqueous solution.[27,28]

CoPt deposits with high cobalt content (76 and 77 at. % of Co, respectively) were obtained by increasing the [$CoCl_2$] in the aqueous component (microemulsions **II** and **III**). A greater amount of deposit than in microemulsion **I** was obtained for the same deposition charge, whose reveals an increase of the efficiency of the process, as a consequence of the lower proportion of platinum in the deposits. Fig. 5a and 5b show CoPt nanoparticles (tending to hexagonal shape) of around 3 nm from microemulsion **II** and around 4 nm from microemulsion **III.** In all cases, the size of the nanoparticles is in the order of the aqueous droplets determined for similar *w/o* microemulsions. [29, 30]

Deposits obtained from microemulsion **III** and **IV** are compared (Fig. 5b and 5c) in order to establish the template effect of the percolated *w/o* and bicontinuous microemulsions. Both microemulsions contain the same [$CoCl_2$] in the aqueous component (*w*), but different proportion of *w* in the microemulsion, as the manner that **III** is a percolated *w/o* microemulsion and **IV** is a bicontinuous one. In both cases the same composition (77 at. % of Co) of the CoPt deposits was obtained, but monodisperse nanoparticles around 4 nm were obtained from percolated microemulsion **III** (Fig. 5b) whereas branched nanostructures were obtained from bicontinuous microemulsion **IV** (Fig. 5c), as it is expected for their intrinsic structure. The proportion of aqueous component in the microemulsion conditions its structure and, therefore, the corresponding deposit structure. For percolated microemulsions (**I, II, III**), the presence of overlapped or interacting aqueous droplets is expected, and small nanoparticles are formed by electrodeposition, although the first confined nanostructures can slowly join in other of greater size. However, for bicontinuous microemulsions such as **IV**, the initial electrodeposited nanostructures are maintained less easily isolated, leading to less confined branched nanometric structures.

The TEM micrographs exhibit different sets of fringe patterns (Fig. 5) in the observed nanoparticles or nanostructures, from which the crystalline structure can be deduced. The Fast Fourier Transform (FFT) taken from representative regions of the samples let us identify lattice fringes, verified by the Selected Area Electron Diffraction patterns (vg Fig. 4e), leading to d-spacings values of 2.23 Å, 2.11 Å and 2.00 Å, which match perfectly with the (100), (002) and (101) orientations of a CoPt hcp structure, distorted respect to the Co hcp one. Moreover, d-spacings of 4.67, 2.86 and 2.44 Å, corresponding to the (111), (220) and (311) orientations of Co_3O_4-fcc structure were detected. The values of the d-spacings of the hcp-

CoPt phase were greater when the at. % of Pt increase as a consequence of higher Pt incorporation.

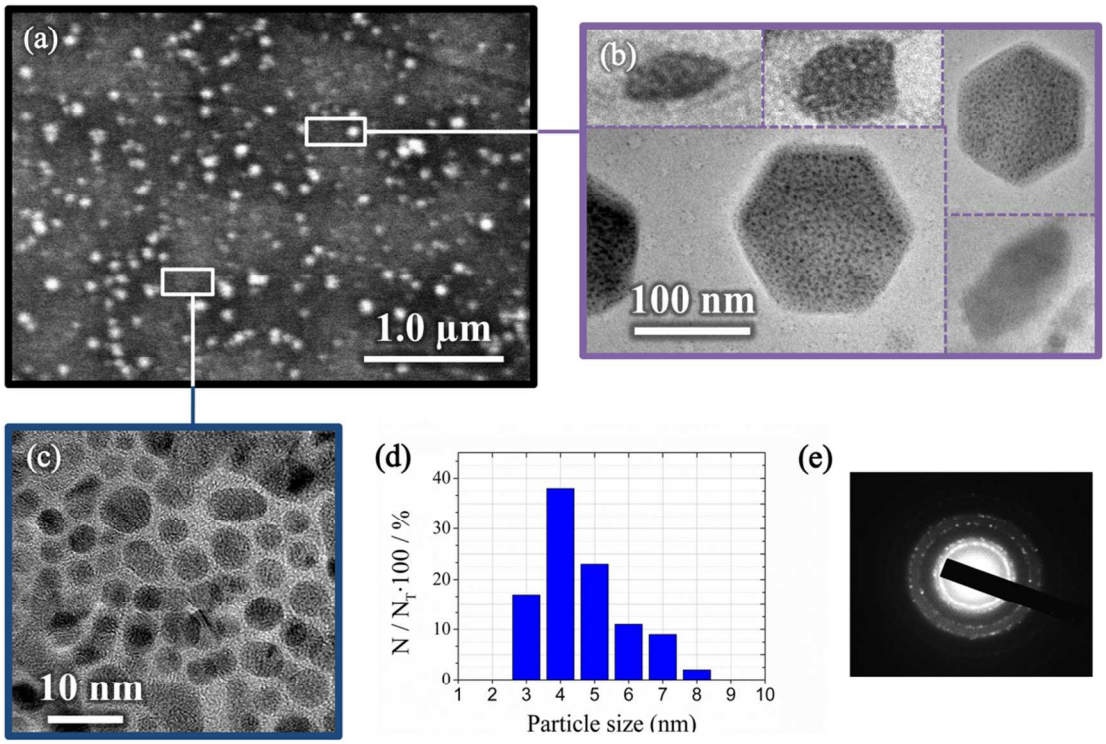

Fig. 4. FE-SEM micrograph (a) and TEM micrographs (b,c) of CoPt deposits obtained in microemulsion **I**. (d) Particle distribution size and (e) selected area electron diffraction of the small particles obtained in microemulsion **I**. Deposition charge: 300 mC cm^{-2}

Journal Name RSCPublishing

ARTICLE

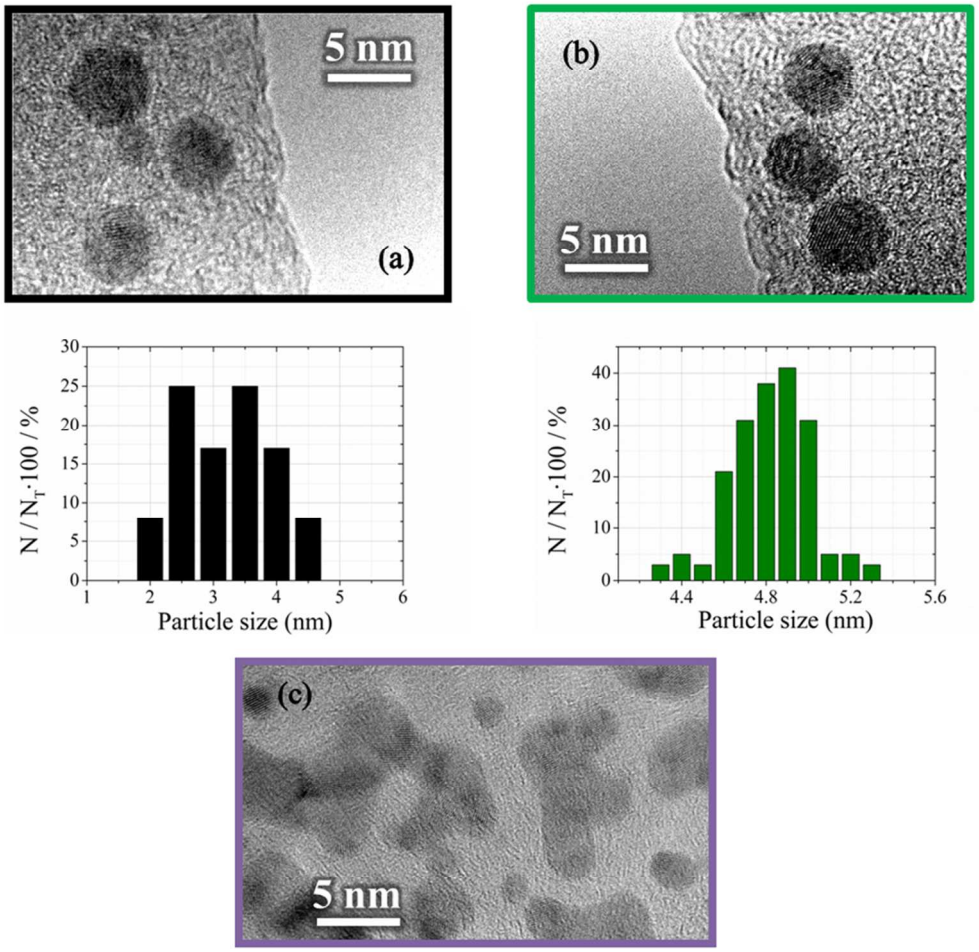

Fig. 5. TEM micrographs of obtained deposits with microemulsions (a) **II**, (b) **III** and (c) **IV**.

4. Conclusion

CoPt electrodeposition from water-in-oil microemulsions formed by aqueous solution of Co (II) and Pt (IV), non-toxic oil (Diisopropyl Adipate) and surfactant (Triton X-100) has been possible. Water-in-oil microemulsions with the maximum conductivity (percolated microemulsions) have been selected to confine the electrodeposition of the CoPt in the interior of the droplets. Bicontinuous microemulsions permit to obtain nanostructures of CoPt following the branched structure of the microemulsion. Non-percolated *w/o* microemulsions present extremely low conductivity and the deposition rate is very low.

CoPt alloy nanoparticles, in the 3-5 nm range, have been obtained, with variable composition as a function of the composition of the aqueous droplets. The modification of the percentage of Co (II) in the droplets modifies the percentage of cobalt in the alloy nanoparticles, but in all cases, nanoparticles are constituted by a Co-Pt alloy with hcp structure and platinum incorporation in the crystalline lattice of the cobalt.

The tested electrochemical method is proposed as a method of growth of metal or alloy nanoparticles on substrates, avoiding overlapping and films formation, because the aqueous droplets of the *w/o* microemulsion maintain the particles isolated during the growth. This method substituted, also, aggressive agents by applied potentials for the reduction process conducting to the nanoparticles.

Acknowledgements

This work was supported by contract CQT2010-20726 from MINECO. The authors wish to thank the Centres Científics i Tecnològics de la Universitat de Barcelona (CCiTUB) for allowing us to use their equipment. The authors also wish to thank the

collaboration of Dra. Gabriela Calderó, Dra. Conxita Solans and Dr. Jordi Esquena from Institut de Química Avançada de Catalunya (IQAC-CSIC) and Centro de Investigación Biomédica en Red en Bioingeniería, Biomateriales y Nanomedicina (CIBER-BBN) for their participation in other previous works that allowed us to do the present study. Substrates have been prepared in IMB-CNM (CSIC), supported by the (CSIC) NGG-258 project. A. S would also like to thank the Ministerio de Educación, Cultura y Deporte for its financial support (FPU grant).

Notes and references

Ge-CPN, Departament de Química Física and Institut de Nanociència i Nanotecnologia (IN^{2}UB), Universitat de Barcelona, Martí i Franquès 1, 08028, Barcelona, Spain.

AUTHOR INFORMATION
Corresponding Author
*Prof. Elisa Vallés
Ge-CPN, Departament de Química Física and Institut de Nanociència i Nanotecnologia (IN^{2}UB), Universitat de Barcelona, Martí i Franquès 1, 08028, Barcelona, Spain.
e-mail: e.valles@ub.edu
Fax: +34 93 4021231

1 D. Zhang, L. Qi, J. Ma and H.Cheng, *Chem. Mater.,* 2002, **14,** 2450.
2 C. Gao, Q. Zhang, Z. Lu and Y. Yin, *J. Am. Chem. Soc.,* 2011, **133** 19706.
3 M. Heurlin, M. H. Magnusson, D. Lindgren, M. Ek, L. R. Wallenberg, K. Deppert and L. Samuelson, *Nature,* 2012, **492,** 90.
4 X. Yu, J. He, D. Wang, Y. Hu, H. Tian, T. Dong and Z. He, *J. Nanopar. Res.,* 2012, **14,** 1260.
5 Q. Huo and J. G. Worden, *J. Nanopar. Res.,* 2007, **9,** 1013.
6 N. Yasui, A. Imada and T. Den, *Appl. Phys. Lett.,* 2003, **83,** 3347.
7 G. Pattanaik and G. Zangari, *J.Electrochem. Soc.*, 2006, **153,** C6.
8 J Casals-Terré, M. Duch, J. A. Plaza, J. Esteve, R. Pérez-Castillejos, E. Vallés and E. Gómez, *Sensor. Actuator.*, 2008, **147,** 600.
9 E. Gómez, E. Pellicer, M. Duch, J. Esteve and E. Vallés, *Electrochim. Acta*, 2006, **51** 3214.
10 M. Duch, J. Esteve, E. Gómez, R. Pérez-Castillejos and E. Vallés, *J. Micromech. Microeng.*, 2002, **12,** 400.
11 Y. Peng, T. Cullins, G. Mobus, X. Xu and B. Inkson, *Nanotechnology., 2007,* **18,** 485704.
12 Y. Dahmane, L. Cagnon, J. Voiron, S. Pairis, M. Bacia, L. Ortega, N. Benbrahim and A. Kadri, *J. Phys. D: Appl. Phys.,* 2006, **39** 4523.
13 L. Cagnon, Y. Dahamane, J. Voiron, S. Pairis, M. Bacia, L. Ortega, N. Benbrahim and A. Kadri, *J. Magn. Magn. Mater.*, 2007, **310,** 2428.
14 I. Danielsson and B. Lindman, *Colloid. Surface*, 1981, **3,** 391.
15 M. P. Pileni, Langmuir, 1997, **13,** 3266.
16 M. A. López-Quintela, C. Tojo, M. C. Blanco, L. García Rio and J. R. Leis, *Curr. Opin. Colloid. In.*, 2004, **9**, 264.
17 V. Uskokovic and M. Drofenik, *Adv. Colloid. Interfac.,* 2007, **133,** 23.
18 C. Aubery, C. Solans and M. Sánchez-Domínguez, *Langmuir*, 2011, 27**,** 14005.
19 N. Zhou, F. S. Bates and T. P. Lodge, *Nano Lett., 2006,* **6,** 2354.
20 W. Worakitkanchanakul, T. Imurab, T. Fukuokab, T. Moritab, H. Sakaia, M. Abea, R. Rujiravanitd, S. Chavadejd, H. Minamikawae and D. Kitamotob, *Colloid. Surface. B., 2009,* **68,** 207.
21 F. Lichterfeld, T. Schmeling and R. Strey, *J. Phys. Chem.*, 1986, 90**,** 5762.
22 J. K. Holmberg, *J. Colloid. Interf. Sci.,* 2004, **274,** 355.
23 C. Destree and J. B. Nagy, *Adv. Colloid Interfac.*, 2006, **123,** 353.
24 A. Serrà, E. Gómez, G. Calderó, J. Esquena, C. Solans and E. Vallés, *Electrochem. Commun.*, 2013, **27,** 14.
25 A. Serrà, E. Gómez, G. Calderó, J. Esquena, C. Solans and E. Vallés, *Phys. Chem. Chem. Phys.*, 2013, **15,** 14653.
26 A. Serrà, E. Gómez, G. Calderó, J. Esquena, C. Solans and E. Vallés, *J. Electroanal. Chem.*, 2014, **720-721,** 101.
27 M. Cortés, E. Gómez and E. Vallés, *Electrochem. Commun.*, 2010, **12,** 132.
28 D. Desai, D. E. Turney, B. Anantharaman, D. A. Steingart and S. Banerjee, *J. Phys. Chem. C*, 2014, **118**, 8656.
29 R. Najjar and C. Stubenrauch, *J. Colloid. Interf. Sci.*, 2009, **331,** 214.
30 L. M. Magno, W. Sigle, P. A. Van Aken, D. G. Angelescu and C. Stubenrauch, *Chem. Mater.,* 2010, **22,** 6263.